Direct Observation of Nuclear Rearrangement in Molecules

Z. Vager,$^{(1),(2)}$ T. Graber,$^{(1),(3)}$ E. P. Kanter,$^{(1)}$ and D. Zajfman$^{(2)}$
$^{(1)}$*Physics Division, Argonne National Laboratory, Argonne, Illinois 60439*
$^{(2)}$*Department of Nuclear Physics, Weizmann Institute of Science, Rehovot, 76100, Israel*
$^{(3)}$*Department of Physics, University of Illinois at Chicago, Chicago, Illinois 60680*
(Received 26 February 1993)

The first direct experimental observation of an intramolecular reaction path going through a transition state is reported. The results of a Coulomb explosion imaging experiment for cold $CH_4{}^+$ molecular ions show the intermediate conformations between permutationally equivalent structures of this molecule. Comparison with a theoretical prediction of the corresponding reaction path is given and the agreement is satisfactory.

PACS numbers: 35.20.Bm

Optical spectroscopy has been extremely successful in deriving the structure of rigid or "semirigid" molecules [1-5]. Spectroscopic data, combined with Born-Oppenheimer approximation (BOA) based *ab initio* calculations, are the basis for much of our understanding of molecular structure. In general, the interpretation of spectra depends on model Hamiltonians and, thus, the coupling between quantum calculations and experiments is essential for the conversion of spectral observations into structural parameters. This rigid structural approach starts having difficulties when one deals with floppy systems. Examples of such systems are van der Waals complexes, clusters, and some molecular ions which are characterized by weak binding energies or weak intramolecular forces [6,7]. For such species the interpretation of high resolution spectra is difficult and not always conclusive [8]. Furthermore, once the system includes large internuclear distances such as in reactions, the BOA theoretical framework must be modified. As a consequence, modern reaction dynamics calculations necessarily employ models which are far more sophisticated and extend beyond the BOA [9-12].

Thus, the field of molecular structure in nonrigid systems suffers from the deficiency of interpretational tools for the extraction of structural parameters. It would be desirable to have more direct experimental and theoretical means for obtaining structural information on such systems. The purpose of this Letter is to report on new experimental possibilities for direct measurements of detailed structural features of floppy molecules including intramolecular dynamics.

Concepts such as "reaction paths," "transition states," "intramolecular reactions," and the like are extremely useful in the field of molecular reactions. A semiclassical description is given by Levine and Bernstein [13]: "The key assumption of the theory is that there exists a single configuration of no return, called the *transition state*. Once the system has reached this configuration, it is assumed to proceed further and form the products. That path (on the surface) along which the reactants reach the critical configuration and along which the supermolecule in the transition state 'deforms' to yield the products is the *reaction coordinate*." Several experimental schemes have been used to obtain indirect information on the transition state configuration. Structural information can be inferred from the features observed in the emission spectra of photodissociating molecules [14]. Interpretation of photoelectron spectra provides another means of gaining insight into the transition state of the dissociating neutral species [15]. We present here a new experimental method by which direct information is achieved on an intramolecular reaction path and a transition state. We demonstrate this method for a special case of the ground state permutational isomerization of $CH_4{}^+$.

The vibrational-electronic coupling caused by electronic degeneracies in nonlinear molecules is a common example of BOA breakdown and is known as the Jahn-Teller (JT) effect [16]. $CH_4{}^+$ is one of the simplest systems which exhibits JT distortion in its triply degenerate ground state. A detailed study of a particular reaction path in the ground state of $CH_4{}^+$ has been given by Frey and Davidson [17]. Various stationary points were located on the calculated lowest energy surface and pseudorotations were studied in terms of bond lengths and bond angles. The deduced "reaction path" in terms of bond angle variables (i.e., the six H-C-H angles) for the tunneling from one minimum to another permutationally equivalent minimum is shown in Fig. 1(a). The conformation at the left side of the figure (path phase of $-\pi/2$) has one small bond angle $\angle H_1\text{-}C\text{-}H_4 = 53°$ and a large opposite bond angle $\angle H_2\text{-}C\text{-}H_3 = 127°$. The other four angles are all 113°. This conformation has the symmetry of a group which can be generated by reflections through two planes perpendicular to each other and is customarily symbolized by C_{2v} [4]. The conformation at the right side of Fig. 1(a) (path phase of $\pi/2$) is another permutationally equivalent minimum with a C_{2v} symmetry. Between these minima there is a barrier of about 80 meV with a conformation (path phase of 0) which is invariant under the exchange of protons 1 and 2 and is marked in Fig. 1(a) by C_s [17].

Coulomb explosion imaging (CEI) [18], a relatively new technique for molecular structure determination, is a model-independent method which directly samples the fully correlated many-body nuclear density for both rigid and floppy systems. In the following, we describe how a

0031-9007/93/70(23)/3549(4)$06.00

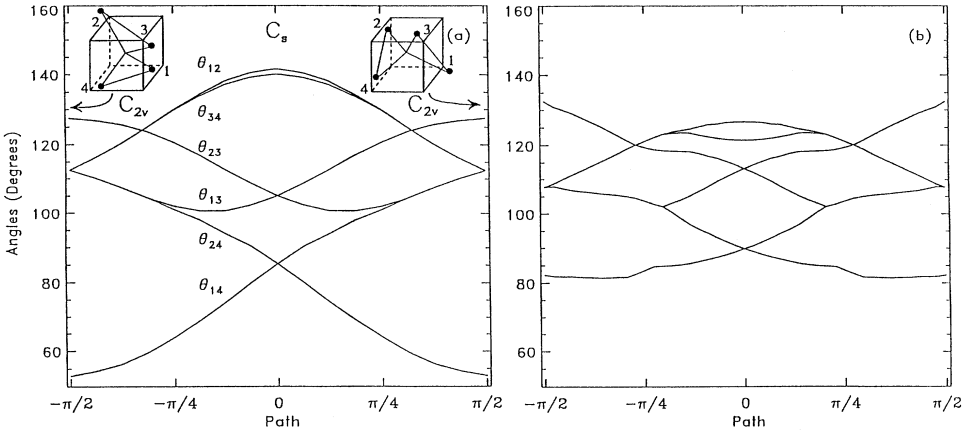

FIG. 1. The H-C-H angles along the reaction path between two equivalent conformations. The abscissa represents a phase angle along the path between these conformations. (a) Theoretical reaction path from [17]. (b) Experimental reaction path (see text).

reaction path, equivalent to the theoretical reaction path shown in Fig. 1(a), is observed directly using the CEI method. For conciseness, we will discuss only the five-dimensional subspace of the measured angular variables. A full treatment of the nine-dimensional CEI data for the structure of CH_4^+ will be published elsewhere.

A persistent technical problem in previous CEI experiments had been the inability to generally prepare fast molecular-ion beams with well defined vibrational excitation [19,20]. Previous CEI experiments on CH_4^+ suffered from this problem [21], thus limiting precise interpretation to a possible reaction path of a mixed molecular ensemble [22]. Recently, an ion source has been developed to produce vibrationally cold molecular ions in the terminal of the Argonne Dynamitron accelerator by implementing a supersonic expansion crossed by an electron beam [23], thus overcoming this problem. Optimal parameters were chosen experimentally for the production of the coldest CH_4^+ ion beam from this source. The molecular ions were accelerated to an energy of 4.5 MeV and, after mass selection, were stripped of their valence electrons by a 0.6 $\mu g/cm^2$ Formvar target [24]. The stripping process occurs in about 10^{-16} s and the remaining atomic ions start Coulomb exploding. For about 40% of all impinging molecular ions, a coincidence of four protons and a carbon ion with charge +3 were collected using two detectors [25,26]. Further details of the experimental procedure may be found in Refs. [26] and [27]. From the information provided by these detectors the simultaneous values of all velocity components may be deduced for each fragment (i.e., a total of 15 components). About 2500 molecular ions were analyzed. For the purpose of studying the topology of the multidimensional nuclear density, the six measured H-C-H angles (between the velocity vectors after the explosion) were used for each CH_4^+ ion. The density in terms of these angles approximates the density in terms of H-C-H angles in the unexploded molecules [18]. Corrections to this approximation will be discussed later, and are unimportant for understanding the method of studying the reaction path.

The six H-C-H angular coordinates depend on five angular normal modes. If we define θ_{ij} as the angle between the H_i-C-H_j fragments for $i,j=1,\ldots,4$ then the following five angular normal modes [17] can be constructed for each measured molecule:

$$\begin{aligned}
B_x &= \sqrt{1/2}(\theta_{12}-\theta_{34}) , \\
B_y &= \sqrt{1/2}(\theta_{24}-\theta_{13}) , \\
B_z &= \sqrt{1/2}(\theta_{14}-\theta_{23}) , \\
E_b &= \sqrt{1/12}[2(\theta_{12}+\theta_{34})-(\theta_{13}+\theta_{14}+\theta_{23}+\theta_{24})] , \\
E_t &= \tfrac{1}{2}(\theta_{13}-\theta_{14}+\theta_{24}-\theta_{23}) .
\end{aligned} \tag{1}$$

Any point in the 5D space (B_x,B_y,B_z,E_t,E_b) can be transformed to the corresponding set of six interbond angles θ_{ij} by noting that any such set of redundant angles must satisfy the additional constraint $\det[\cos(\theta_{ij})]=0$. In this 5D space, the origin represents a regular tetrahedral geometry. Every measured molecule contributes 24 points to the density in this 5D space, representing all the possible permutations of the four experimentally identical protons. Thus, about 60 000 points contribute to the measured ensemble. A procedure for smoothing the statistical fluctuations of the density is used [28] and we refer to this 5D smoothed density as the measured density. Except for some minor Coulomb and target distortions which can be accurately simulated [29], the measured distribution represents the actual ground state nuclear density for the angle variables. Moreover, the measured density represents the square of the nuclear wave function whenever a single electronic potential surface is applicable.

Figure 2(a) shows a cut of the measured density on the (B_y,B_z) plane at $B_x=E_b=E_t=0$. As expected, the regu-

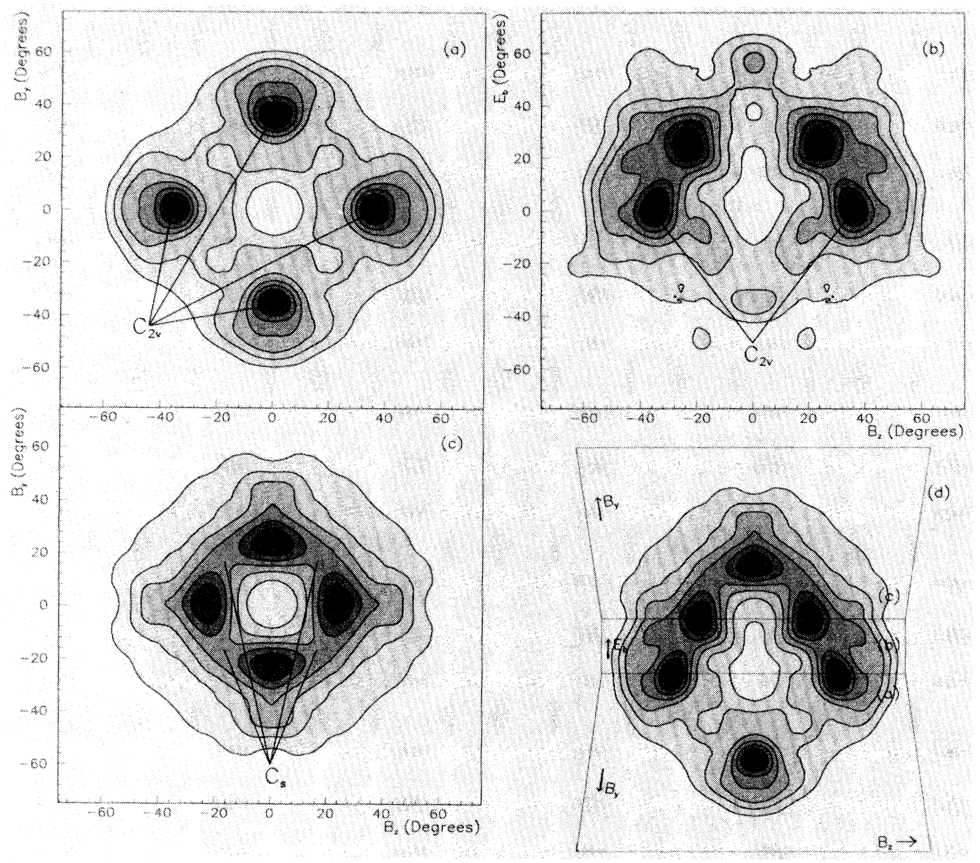

FIG. 2. Two-dimensional cuts from the five-dimensional experimentally measured density (see text) of the angle variables. (a) B_y vs B_z at $B_x=E_b=E_t=0$, (b) E_b vs B_z at $B_x=B_y=E_t=0$, (c) B_y vs B_z at $B_x=E_t=0$; $E_b=25°$. (d) Composite view of the segments of the reaction paths which appear in (a), (b), and (c).

lar tetrahedral structure does not contribute to the density because of the JT symmetry-breaking mechanism. Four prominent equivalent peaks appear symmetrically around the origin on the B_y and B_z axes (and, not shown, two others on B_x). These peaks represent structures of C_{2v} symmetry and are marked as C_{2v} in the figure. The lower and the left peaks have the six θ_{ij} angles given in Fig. 1(b) at the extreme left and right sides, respectively.

Figure 2(b) shows a cut of the measured density on the (B_z,E_b) plane at $B_x=B_y=E_t=0$. The two peaks on the B_z axis from Fig. 2(a) are still present in this view, however, here they are connected through ridges to two new peaks at $E_b\cong 25°$. Each of the two high density regions has two comparable peaks connected via a saddle. The connecting ridges are identified as the experimental reaction paths between the conformations of the peaks. On this plane, any nonzero E_b value lowers the C_{2v} symmetry into a twofold axis C_2 symmetry, which is the symmetry of the new peaks. To complete the experimentally observed pseudorotation picture we show in Fig. 2(c) a cut of the measured density on the (B_y,B_z) plane at $B_x=E_t=0$ but $E_b\cong 25°$ which is where the new peaks appeared in Fig. 2(b). Four prominent equivalent peaks appear symmetrically around the origin on the B_y and B_z axes connected by four saddles. These four peaks, two of which appear in Fig. 2(b) at $E_b\cong 25°$, represent conformations of C_2 symmetry. The saddle points between the peaks are identified as the transition states and marked by C_s. The experimental transition states are true saddle points in 5D, namely, the density is a maximum for every direction except for one, for which it is a minimum. In this plane, all six angles differ from each other, except on the two axes and on the diagonals ($B_y=\pm B_z$) which represent loci of C_2 and C_s conformations, respectively. Figure 2(d) is a perspective view combining the two parallel cuts of Figs. 2(a) and 2(c), and one of the connecting perpendicular planes shown in Fig. 2(b). An equivalent (E_b,B_y) plane at $B_x=B_z=E_t=0$ (not shown) connects the uppermost (C_2) and lowermost (C_{2v}) peaks in Fig. 2(d), which completes the exchange of protons 1 and 2. Thus, we have found a passage of high probability density in 5D configuration space which connects permutationally equivalent peaks to each other. Physically, the experimental data show that the CH_4^+ ground state is unlocalized along connected one-dimensional paths in this space.

For accurate tracing of the reaction path, it is possible to make a computer search in the 5D space which follows the ridges of the measured density. The result of such a search is shown in Fig. 1(b). The qualitative similarity between the theoretically computed reaction path and the experimentally deduced one is evident. Some of the quantitative differences between them can be accounted for by Coulomb distortions such as proton-proton repulsion for small H-C-H angles (this is more pronounced at $\pm\pi/2$ in Fig. 1, where the smallest measured angle is larger by 30° than the theoretical one). As mentioned before, this has been neglected in this simplified analysis.

The reaction paths shown in Figs. 1(a) and 1(b) appear quite similar. However, Fig. 1(a) shows the changes occurring in the H-C-H angles along a reaction path between two equivalent minima where the path is calculated from a model potential surface, while the results shown in Fig. 1(b) are based on the path which follows the maximum probability ridges of the measured density. In both Figs. 1(a) and 1(b), the six H-C-H angles start with a C_{2v} symmetry structure where four equal angles split into two pairs of equal angles lowering the symmetry to C_2 [4]. Further along the path, a bifurcation of each pair occurs. All six H-C-H angles are then unequal until the transition state is reached at path phase equal to zero in Figs. 1(a) and 1(b). After this point, one pair of the four initially equal angles gradually evolves and assumes the role of the largest and the smallest angles in the conformation shown on the right side of Figs. 1(a) and 1(b). All other angles drift toward equality in a fashion symmetrically similar to the left side.

To conclude, we have presented the first detailed model-independent measurement of an isomerization reaction path and transition states using the CEI method. The complete analysis of the data should reveal further significant information on the dynamics of the permutational isomerization of the CH_4^+ ground state, such as additional correlation with C-H bond lengths and the relative densities of conformations. The technique offers a possibility to obtain experimental information, which was unavailable before, on dynamics of floppy molecular systems.

The authors would like to acknowledge the technical help of B. J. Zabransky, R. Amrein, and A. Ruthenberg. We also acknowledge highly valuable discussions with R. Naaman. We wish to thank E. R. Davidson for permission to reproduce Fig. 1(a). D.Z. and Z.V. thank the Minerva Foundation-Munich for financial support. This work was partially supported by the U.S. Department of Energy under Contract No. W-31-109-ENG-38.

[1] G. Herzberg and K. P. Huber, *Molecular Spectra and Molecular Structure* (Van Nostrand Reinhold, New York, 1945).

[2] C. H. Townes and A. L. Schawlow, *Microwave Spectroscopy* (McGraw-Hill, New York, 1955).

[3] H. C. Allen and P. C. Cross, *Molecular Vib-Rotors* (Wiley, New York, 1963).

[4] E. B. Wilson, Jr., J. C. Decius, and P. C. Cross, *Molecular Vibrations* (McGraw-Hill, New York, 1955).

[5] P. R. Bunker, *Molecular Symmetry and Spectroscopy* (Academic, New York, 1979).

[6] *Structure and Dynamics of Weakly Bound Molecular Complexes*, edited by A. Weber, NATO ASI Series, Vol. 212 (Reidel, Boston, 1987).

[7] R. E. Miller, Science **240**, 447 (1988).

[8] D. J. Nesbitt and R. Naaman, J. Chem. Phys. **91**, 3801 (1989).

[9] M. H. Alexander, W. J. Werner, and D. J. Dagdigian, J. Chem. Phys. **89**, 1388 (1988).

[10] M. Shapiro and H. Kaplan, J. Chem. Phys. **71**, 2182 (1979).

[11] G. G. Balint-Kurti, J. Chem. Phys. **84**, 4443 (1986).

[12] M. H. Alexander and B. Pouilly, J. Chem. Phys. **90**, 5373 (1989).

[13] R. D. Levine and R. B. Bernstein, *Molecular Reaction Dynamics and Chemical Reactivity* (Oxford Univ. Press, New York, 1987).

[14] See, for example, D. Imre, J. L. Kinsey, A. Sinha, and J. Krenos, J. Phys. Chem. **88**, 3956 (1984).

[15] R. B. Metz *et al.*, J. Phys. Chem. **94**, 1377 (1990).

[16] H. A. Jahn and E. Teller, Proc. R. Soc. London A **161**, 220 (1937).

[17] R. F. Frey and E. R. Davidson, J. Chem. Phys. **88**, 1775 (1988).

[18] Z. Vager, R. Naaman, and E. P. Kanter, Science **244**, 426 (1989).

[19] A. Faibis, E. P. Kanter, L. M. Track, E. Bakke, and B. J. Zabransky, J. Phys. Chem. **91**, 6445 (1987).

[20] Z. Vager and E. P. Kanter, J. Phys. Chem. **93**, 7745 (1989).

[21] Z. Vager, E. P. Kanter, G. Both, P. J. Cooney, A. Faibis, W. Koenig, B. J. Zabransky, and D. Zajfman, Phys. Rev. Lett. **57**, 2793 (1986).

[22] Z. Vager, in *The Structure of Small Molecules and Ions*, edited by R. Naaman and Z. Vager (Plenum, New York, 1987), p. 105.

[23] T. Graber, D. Zajfman, E. P. Kanter, R. Naaman, Z. Vager, and B. J. Zabransky, Rev. Sci. Instrum. **63**, 3569 (1992).

[24] G. Both, E. P. Kanter, Z. Vager, B. J. Zabransky, and D. Zajfman, Rev. Sci. Instrum. **58**, 424 (1987).

[25] A. Faibis, W. Koenig, E. P. Kanter, and Z. Vager, Nucl. Instrum. Methods Phys. Res., Sect. B **13**, 673 (1986).

[26] A. Belkacem, A. Faibis, E. P. Kanter, W. Koenig, R. E. Mitchell, Z. Vager, and B. J. Zabransky, Rev. Sci. Instrum. **61**, 946 (1990).

[27] D. Zajfman, A. Belkacem, T. Graber, E. P. Kanter, R. E. Mitchell, R. Naaman, Z. Vager, and B. J. Zabransky, J. Chem. Phys. **94**, 2543 (1991).

[28] The following procedure was used for the determination of a smooth 5D density in the space defined by Eq. (1). Each measured point was smeared by a 5D isotropic Gaussian with a standard deviation of 5°. The smoothed density was determined by the sum of these Gaussian distributions.

[29] D. Zajfman, T. Graber, E. P. Kanter, and Z. Vager, Phys. Rev. A **46**, 194 (1992).

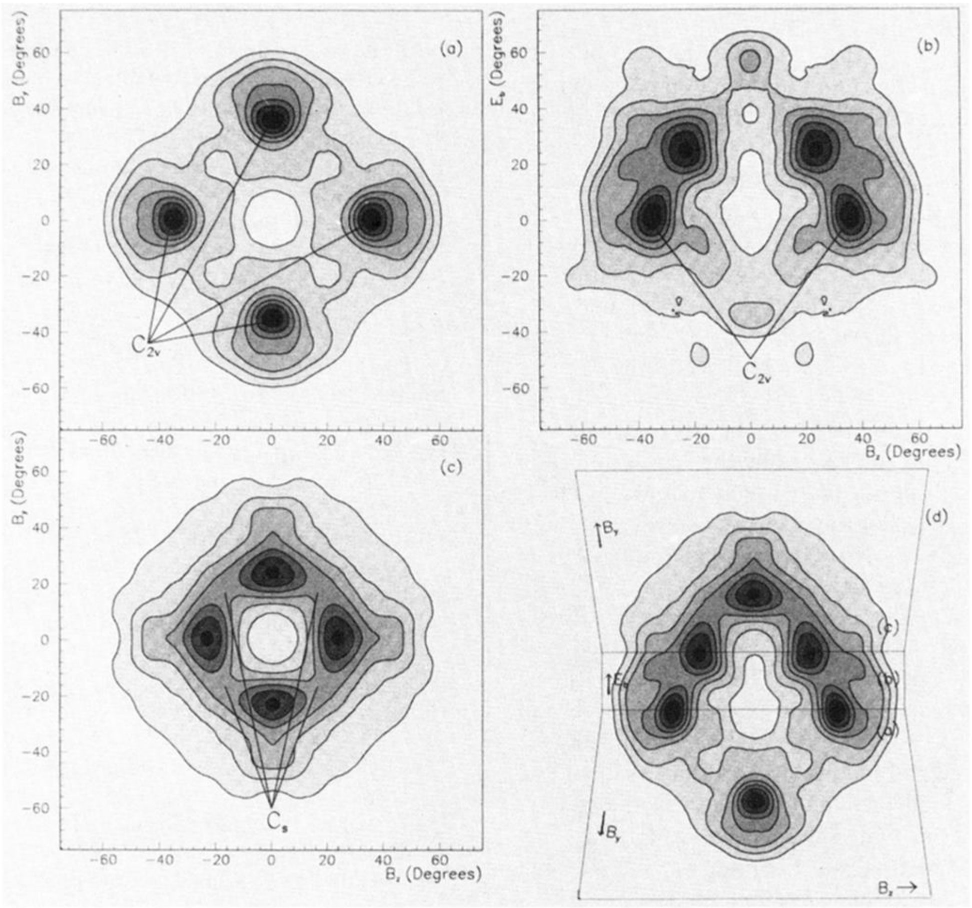

FIG. 2. Two-dimensional cuts from the five-dimensional experimentally measured density (see text) of the angle variables. (a) B_y vs B_z at $B_x = E_b = E_t = 0$, (b) E_b vs B_z at $B_x = B_y = E_t = 0$, (c) B_y vs B_z at $B_x = E_t = 0$; $E_b = 25°$. (d) Composite view of the segments of the reaction paths which appear in (a), (b), and (c).